IEEE Access
Multidisciplinary | Rapid Review | Open Access Journal

Received August 6, 2019, accepted August 12, 2019, date of publication August 16, 2019, date of current version August 30, 2019.

Digital Object Identifier 10.1109/ACCESS.2019.2935754

Effect of the Speckle Size on the Quality of Speckle Pattern in DSPI System

ZHISONG LI[1], PING ZHONG[1,2], XIN TANG[1], JIAYAO LING[2], JIAWEI CHEN[2], AND GUOXING HE[2]

[1]College of Information Science and Technology, Donghua University, Shanghai 201620, China
[2]Department of Applied Physics, Donghua University, Shanghai 201620, China

Corresponding author: Ping Zhong (pzhong937@dhu.edu.cn)

This work was supported in part by the National Natural Science Foundation of China under Grant 51575099 and Grant 51975116, in part by the Fundamental Research Funds for the Central Universities, and in part by the Graduate Student Innovation Fund of Donghua University under Grant GUSF-DH-D-2019088.

ABSTRACT In order to detect the deformation and strain of materials accurately, the key is to obtain the phase information caused by dynamic loading in digital speckle pattern interferometry (DSPI). In this paper, the evaluation method of quality of the speckle pattern in DSPI system is proposed, and the influence of the size of speckle grain on the stability and contrast of speckle pattern is discussed. And then, the strain detection experiments of inactive and bioactive materials are provided with different aperture slit size under the same detection conditions. The size of speckle grain has an important influence on the quality of speckle pattern. For strain detection of inactive materials, using the small size of speckles can obtain higher quality speckle pattern under the condition of satisfying the Nyquist theorem and spectral separation. For active biomaterials, non-structural factors easily induce the instability of speckle pattern, which leads to the de-correlation of between pre-deformation and post-deformation speckle pattern. So the compromise between the stability and the information capacity of speckle images should be considered in the selection of speckle size. Experiments show that the optimum size of speckles used for strain detection active biomaterials is larger than that of inactive biomaterials under the same conditions in the same DSPI system.

INDEX TERMS Speckle stability, image contrast, de-correlation, speckle size, strain distribution detection.

I. INTRODUCTION

The strain detection of bioactive materials is becoming more and more important. For example, in the process of prosthetic limb design and replacement, there are various challenges in improving prosthetic devices for patients with lower limb amputation and total joint replacement. One of the major problems with existing equipment is that it cannot be applied to wet and active biomechanical interface at the bone surface. Determining the strain distribution and assessing potential stress mismatches at the interface is critical to prevent misalignment, loosening, infection in the interfacial space, or induction of osteonecrosis [1]. Although computer-aided design (CAD) software and finite element modeling are useful for the evaluation of bone deformation and strain [2]–[4], these models need to be verified by precise boundary conditions and material property parameter. What is more, due to the bone is a non-uniform anisotropic material [5], it is also necessary to measure the microscopic strain to understand the biomechanical of the bone interface. So it is very important to carry out experimental measurements on the deformation and strain at the bone interface.

Non-destructive testing (NDT) is a technique used to evaluate the strain of a structure or product without causing damage [6]. Optical NDT techniques have such advantages as real-time inspection, whole-field test, non-contact measurement, and high-sensitivity [7], and have been widely used in deformation measurement. The optical NDT mainly includes holographic interferometry (HI) [8], digital speckle pattern interferometry (DSPI) [9], [10], digital image correlation (DIC) [11], etc. Unfortunately, the difficulty in obtaining high quality speckle patterns blocks the application of optical NDT technology to biomaterial detection.

DSPI, originally called as electronic speckle pattern interferometry (ESPI) [12], is considered as the most reliable method for measuring microscopic deformation, strain and

The associate editor coordinating the review of this article and approving it for publication was Mu Zhou.

even temperature [13]–[17] and its application is regarded as the new era of NDT strain detection [18]–[25]. However, the DSPI cannot be directly applied to strain detection of bioactive materials, especially in physiological conditions. One of the biggest challenges is the de-correlation of speckle patterns caused by instability [26]. Unlike the inactive materials (for example, metal materials, dry biomaterial, etc.), the bioactive materials have the random motion of water molecule, which makes distribution of water molecule on the measured surface constantly change with the change of external environment, and it will lead to the instability of speckle pattern, which will lead to serious noises in phase map from pre-deformation and post-deformation speckle pattern. With the increase of speckle instability, the noise caused by the de-correlation becomes more and more serious, eventually the phase information being submerged in the noise. There are some reports on how to improve the correlation of laser speckle patterns [27]–[29]. Gaudette measured the surface deformations of epicardial heart based on the DSPI technology, in which he placed carbon-silicon particles on the heart surface to change the characteristics of the active surface [30]. Ping achieved the strain measurement of the bone active surface by introducing phosphate buffer saline medium imaging environment to reduce the influence of wet surface [31]. Although these methods can restrain the de-correlation of speckle patterns caused by the activity of the detected object to a certain extent, they are still not of universal significance. How to use the existing DSPI detection system to obtain the best speckle patterns is one of the most critical technologies for strain detection.

At present, little consideration is given that the size of speckle grain how affects stability of speckle patterns in the design of the DSPI system which is suitable for biomaterials strain detection, and few discussion of the size of speckle is found in the related research fields, such as the effect of speckle size on random phase measurement error in non-physiological conditions [32] and contrast imaging in physiological conditions [33], [34]. Considering that the size of aperture slit in DSPI can change the size of speckles, the influence of speckle size on the quality of speckle patterns is studied by changing the size of aperture slit in this paper. The comparative experiments of strain detection of inactive materials and active biomaterials have proved the influence of speckle size on the quality of speckle patterns acquired by different detection objects in design of DSPI system.

The paper is structured as following: In section II, the experimental device is introduced and the effect of speckle/pixel ratio on image quality in DSPI system is analyzed. In section III, the evaluation method of speckle image quality is proposed. Section IV the influence of the size of speckles on the quality of speckle pattern is analyzed by changing the size of the aperture slit and in the section V, the strain detection experiments of inactive and bioactive materials are provided with different aperture slit size under the same detection conditions in DSPI, and then the conclusion is given in section VI.

II. EXPERIMENTAL DEVICE AND THE REQUIREMENTS FOR THE SPECKLE/PIXELSIZE RATIO

A. THE SCHEMATIC OF THE EXPERIMENTAL SETUP FOR SPECKLE IMAGE ACQUISITION

In this paper, we take the metal aluminium plate and fresh bones as the research object and design a DSPI detection system based on spatial phase shift technology to explore the influence of the size of speckles on the quality of speckle patterns. Figure 1 show the schematic of the experimental setup for speckle patterns acquisition generated in time by the illumination of the samples using a solid-state laser beam (532.8nm, 0-2.5W). The experimental system mainly consists of DSPI imaging unit, loading device and computer system, etc.

In Figure 1, the solid-state laser emitted a beam with a wavelength of 532.8nm. According to the requirements of DSPI imaging system, the coherent light source is split into a reference beam (5/100) and an object beam (95/100) by

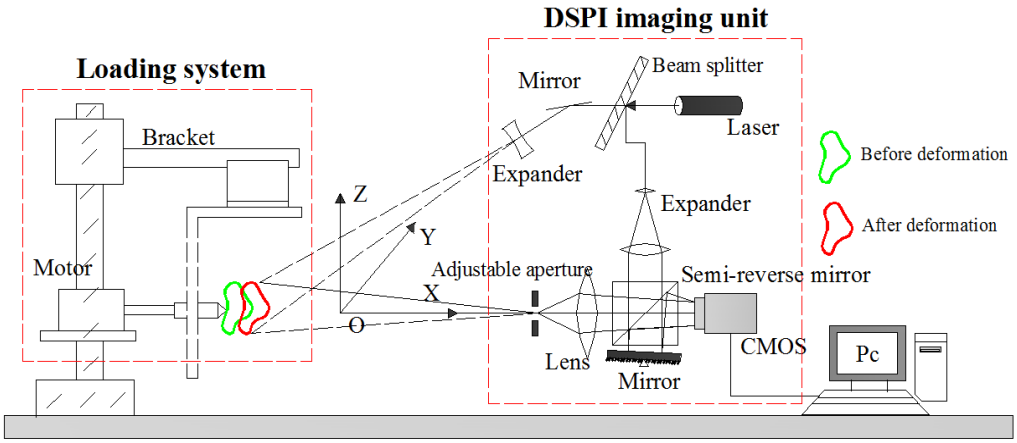

FIGURE 1. The schematic of the experimental setup for speckle patterns acquisition with DSPI.

a beam splitter. The object beam is expanded by a beam expander (BE) and then illuminates the object. The diffused object light reflected from the object and goes through a slit aperture, imaging lens (the focal length is 100mm), semi-reverse mirror and arrives at the CMOS (Basler pixel size 3.45μm $\times$ 3.45μm, resolution of 2448 $\times$ 2048 pixels, sampling rate 23 fps). On the other hand, the reference beam goes through another beam expander (BE), adjustable attenuator, semi-reverse mirror and reaches tilting mirror. After being reflected by the tilting mirror, the speckle pattern generates as a result of the interference between the reference beam and object beams is recorded by a CMOS camera. The tilting mirror introduces a spatial carrier in the x-axis of the reference beam which allows the Fourier method to retrieve the optical phase. The angle of the tilting mirror is related to the pixel size of the CMOS camera's sensor and the illumination wavelength.

The electric load-driven system includes voice coil motor, clamping device, loading tip, loading control system, etc. the minimum loading displacement of electric loading system is 0.5μm. After the samples are fixed, the loading system generates a fixed displacement to produce a strain. The adjustable aperture silt size can be set from 0.05 mm to 6.2 mm. In the designed DSPI, the amplification factor of the optical system equal to 0.1207.

B. METHOD OF CONTROLLING SPECKLE SIZE

In DSPI, the quality of the speckle pattern must be considered as the first step before phase data processing for dynamic loading strain detection, as is notably necessary in biological samples where its activity is very high under physiological conditions. The speckle pattern is the carrier of information in the DSPI system. Speckle attributes not only affect the quality of speckle pattern, but also affect its stability [35]. Especially when the DSPI system is applied to high-precision strain detection of bioactive materials, speckle size plays a key role in the performance of the detection system. In the DSPI system, the size of the individual speckle is not determined by the structure of the surface producing it or by the scattering center's distribution [36]. It is determined entirely by the f-number of the optical system used to observe the speckle pattern. The relationship between the speckle size and the f-number (F) of the compact macro lens is given by the formula (1) [37]:

$$r_{\text{speckle}} = 1.22\lambda(1 + M) * F \tag{1}$$

where, M is the optical magnification, λ is the wavelength of the laser, and F is the f-number of the lens. The F is determined by the following formula (2) [38].

$$F = {}^{f}\!/_{D} \tag{2}$$

where, D is the size of the aperture slit and f is the focal length of the imaging lens. For optical system designed in DSPI, laser wavelength λ, the focal length f and the magnification M are fixed, therefore, the size of speckles can be controlled by changing the size of the aperture silt.

C. REQUIREMENTS FOR THE SPECKLE-PIXEL SIZE RATION IN DSPI SYSTEM

The purpose of selecting the optimum speckle size in the DSPI system is to maximize the information of phase image and to improve the spatial resolution of speckle image [39]. Thus in the paper, whether the optimal speckle image can be obtained is explored by adjusting the aperture slit size. In order to better analyze the influence of speckle size on system performance, we propose the concept of **speckle-pixel size ratio**, and use the sampling theorem to analyze the constraints of speckle size in DSPI. The terms such as speckle-pixel size matching [40] or speckle-pixel size ratio [41] are defined as a universal parameter in many speckle imaging systems. According to the Nyquist theorem, the speckle-pixel size ratio should be greater than 2 [42]. However, the higher the speckle-pixel size ratio is, the less information the speckle pattern has in a DSPI system. Considering that there are many factors affecting the quality of phase image in process of strain detection, how to choose the speckle/pixel ratio is a complex process. Therefore, it is not possible to determine the optimal speckle size for obtaining high quality speckle image only by using Nyquist theorem. The Nyquist theorem is only the basic requirement for the selection of speckle size.

In this paper, strain detection is based on DSPI system, and the image acquired by CMOS is the sum of vectors from the reference light and object light. Size of speckle which is formed by object light can be determined by the formula (1). Owing to relatively uniform parallel beam, the reference beam only changes the overall light intensity on the CMOS and has no effect on the distribution of speckles. So the reference light will not affect the stability of speckles in DSPI. Particularly, for the moment of inertia (IM) which is based on the variety of the Time History Speckle image (THSP). The introduction of reference light only changes the spatial position of the co-occurrence matrix (COM) along the diagonal line, but is does not change the value of *IM*.

In addition, for the DSPI system based on space phase shift technology, the aperture slit size not only affects the size of speckle grain, but also is closely related to the carrier frequency of the system. The choice of carrier frequency is one of the most basic necessary procedures and must meet the following requirements: a) the carrier frequency should be large enough to achieve complete separation of all spectrums; b) all valid spectral frequencies should not exceed the maximum spatial frequency of the camera. So there is a constraint relationship as shown below for DSPI system [43].

$$4f_{\text{s}} \leq f_{\text{carrier}} \leq \frac{2f_{\max}}{3} \tag{3}$$

where, f_s represents the spatial resolution of the speckle image, which can be expressed as $f_s = 1/2r_{\text{speckle}}$. f_{max} is the maximum spatial frequency of camera. It can be expressed as $f_{max} = 1/2d_{pixel}$, and d_{pixel} is pixel size. Then, equation (3) can be written as $r_{speckle} \geq 6\ d_{pixel}$. This indicates that the speckle-pixel ratio should be greater than 6.

According to the designed experimental system, the radius of speckle grains is controlled by the aperture slit size. The relationship between the aperture size and the speckle-pixel ratio can be obtained, as shown in the table 1.

TABLE 1. Speckle grain parameters of experimental system under different aperture slit sizes.

Serial number	Aperture slit size (mm)	Speckle particle size (μm)	Pixel size (μm)	Speckle-pixel size ratio
1	6.2	11.55	3.45	3.349
2	5.0	14.34	3.45	4.15
3	4.2	17.07	3.45	4.94
4	3.6	19.92	3.45	5.77
5	3.2	22.41	3.45	6.49
6	2.5	28.68	3.45	8.31
7	2.1	34.15	3.45	9.89
8	1.8	39.84	3.45	11.54
9	1.5	47.81	3.45	13.85
10	1.2	59.76	3.45	17.32
11	1.0	71.71	3.45	20.78
12	0.8	89.64	3.45	25.98
13	0.7	102.45	3.45	29.69
14	0.6	119.53	3.45	34.64
15	0.5	143.43	3.45	41.57
16	0.4	179.29	3.45	51.97
17	0.3	239.06	3.45	69.29
18	0.2	358.59	3.45	103.94
19	0.1	717.18	3.45	207.88
20	0.05	1434.37	3.45	415.76

For observing the relationship between the aperture slit size and the speckle-pixel size ratio, the corresponding curve is drawn according to the Table 1, and the result is shown in Figure 2.

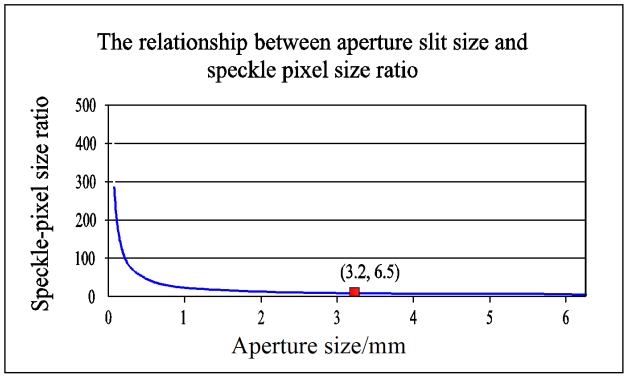

FIGURE 2. Relationship between apertures slit size and speckle-pixel size ratio.

The Nyquist theorem is usually used as the most basic rules for speckle size in DSPI system. In the design of DSPI system, the corresponding aperture slit size should be less than 20mm according to the Nyquist theorem. Furthermore, for DSPI system based on spatial phase shifting, the spectral separation is met only when the speckle-pixel ratio is greater than 6, in which the corresponding aperture slit size should be less than 3.2 mm. So, taking these two aspects into consideration, the following studies only need to be considered when the width of the aperture slit is less than 3.2mm.

III. EVALUATION OF SPECKLE IMAGE QUALITY

Acquiring accurate phase information is the key to strain detection using DSPI technology. The detection of phase information depends on the quality of speckle pattern before and after deformation. The stability and the contrast of speckle pattern are the most critical indicators. The speckle stability directly determines the correlation of speckle images before and after strain, and affects phase image quality [31]. Speckle image contrast directly affects the quality of the speckle image [44]. In this section, we mainly discuss the stability evaluation and the contrast calculation of speckle pattern.

A. STABILITY EVALUATION OF SPECKLE PATTERN

Moment of inertia (IM) is based on the construction and analysis of Time of the History Speckle image (THSP) [45]. The moment of inertia method, often abbreviated as IM, has been considered to be the most effective stability evaluation method, which can return dimensionless data to characterize low or high stability of the observed material based on changes in the THSP image [46]. For the assessment of speckle stability, a certain number of time series speckle images were recorded to monitor the same area. Then, the same rows from the time series images are selected to construct a new image. The constructed image is called THSP. In the THSP, the rows pixels indicate different spatial location points, and the columns represent the change of light intensity in the time domain at the same location.

After the THSP image is constructed, its corresponding co-occurrence matrix (COM) and moment of inertia (IM) can be obtained separately. Among them, the co-occurrence matrix can be built by the following formula [47].

$$COM = \left[N_{ij}\right], \tag{4}$$

In the formula above, i and j represent the gray value of the pixels, and N represents the number of times j follows i in the THSP.

The COM is built by the calculation of N, in which the ith row and jth column elements are value of N. So, if the COM is from a static sample, it will only have non-zero elements on its diagonal line. In contrast, if the COM is constructed by speckle images from active sample, its COM will appear to be a cloud pattern near the diagonal line.

The moment of inertia method is capable of calculating the stability value of a sample by the co-occurrence matrix. The corresponding calculation formula is as follows [48].

$$IM = \sum_{i,j} M_{ij}(i-j)^2, \tag{5}$$

where, M_{ij} represents the probability of occurrence of N_{ij}, and the expression of M can be written as:

$$M_{ij} = N_{ij} / \sum_{j} N_{ij}, \tag{6}$$

The obtained IM value is based on a series of time domain speckle images, so the IM value can be used to indicate the

degree of stability of speckle image. And the smaller the IM value is, the more stable the speckle is.

B. QUALITY OF SPECKLE PATTERN

In the DSPI detection system, the speckle pattern is used as the information carrier of the strain caused by dynamic loading, so it is very necessary to evaluate the quality of speckle pattern. Contrast is an important index for evaluating image quality and one of the effective methods to evaluate the contrast is calculating the power spectrum width [49]. The power spectrum is a frequency domain variable that shows the spectral intensity distribution over spatial frequencies and reflects the energy corresponding to different frequencies in the frequency domain [50]. Therefore, with the deterioration of image quality, the image details became blurred which also narrow the width of the power spectrum. So width of the power spectrum can be used to evaluate the amount of information in the speckle image [51]. The power spectrum calculation method is as follows [52].

$$F(u,v)=\sum_{x=0}^{M-1}\sum_{y=0}^{N-1}f(x,y)\exp\left[-j2\pi\left(\frac{ux}{M}+\frac{vy}{N}\right)\right]u\Delta v \quad (7)$$

where, $F(u,v)$ is the Fourier transforms of the speckle images, and $f(x,y)$ is the speckle image, M and N are the width and height of speckle image, respectively.

$$\Gamma(u,v)=10\lg\frac{F(u,v)\times F^{*}(u,v)}{MN} \quad (8)$$

where, $\Gamma(u,v)$ is the power spectrum distribution function, $F^{*}(u,v)$ is the conjugation of $F(u,v)$, $M\times N$ is the size of the image $F(u,v)$.

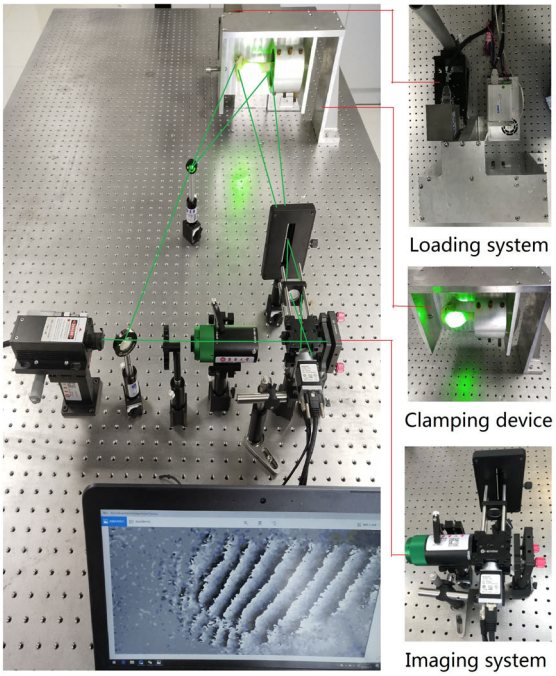

FIGURE 3. Experimental set-up for evaluating the influence of the speckle size on the quality of speckle patterns.

For measuring the contrast accurately, we need to specifically define the concept of power spectrum width. Generally speaking, if the power spectrum comes from a realistic signal, its energy distribution will show a gradual upward or downward trend along the frequency. So we define a boundary between the region of substantial energy and minimal energy. In the paper, the half-power point is defined as the boundary where the power is half the maximum value in the signal [49]. Thus, the power spectrum width can be obtained, and it is used to characterize the contrast of speckle images.

IV. EFFECT OF THE SIZE OF SPECKLES ON QUALITY OF SPECKLE PATTERN COME FROM BIOACTIVE MATERIALS

In the paper, a series of experiments were carried out to explore the effect of size of speckles on the stability and contrast of speckle patterns from bioactive materials.

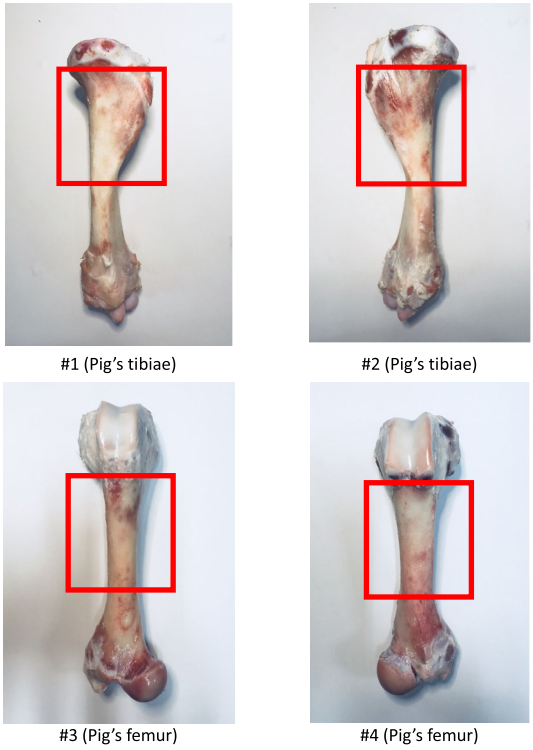

FIGURE 4. Active bone samples (Sample number: #1~#4).

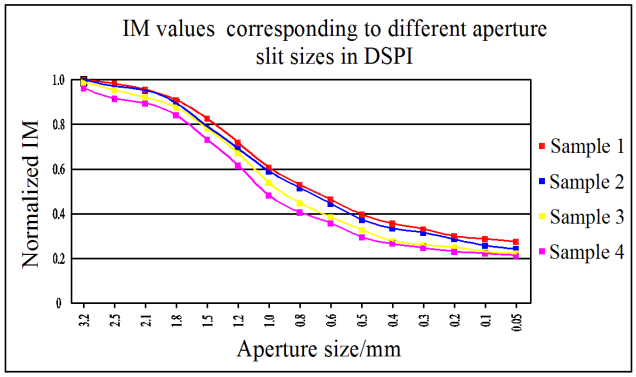

FIGURE 5. *IM* values corresponding to different aperture slit sizes in DSPI.

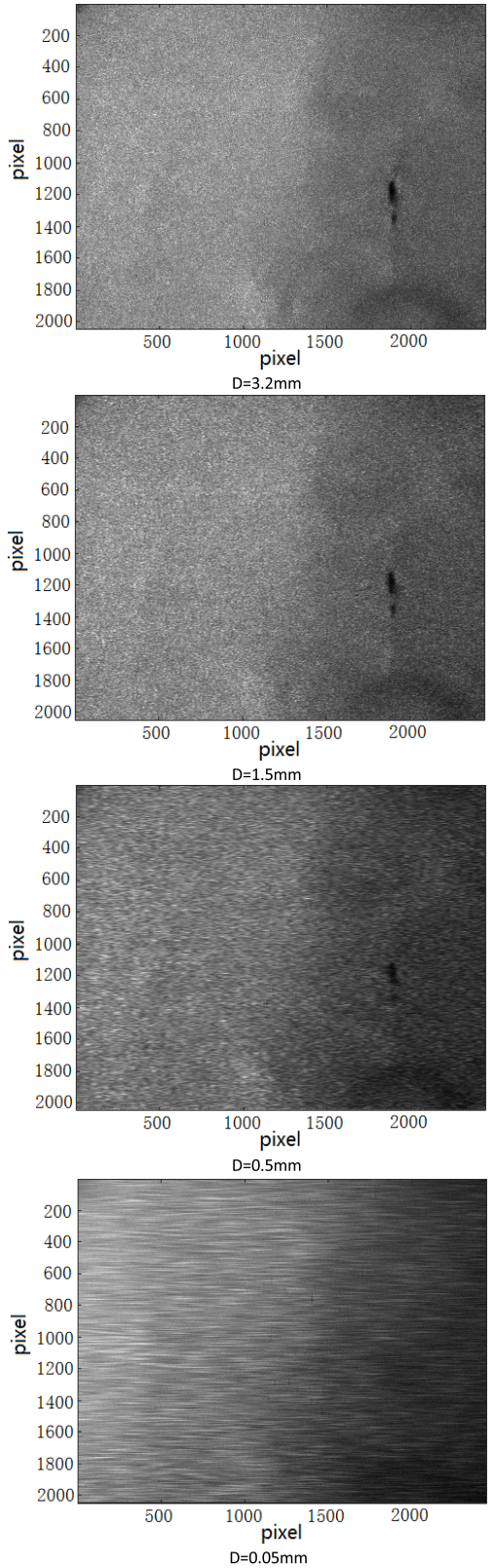

FIGURE 6. The laser speckle patterns obtained from different aperture slit sizes.

According to the schematic of the experimental setup shown in Fig.1, the experimental set-up used to acquire the speckle patterns is shown in Figure 3. In the experiment, the speckle

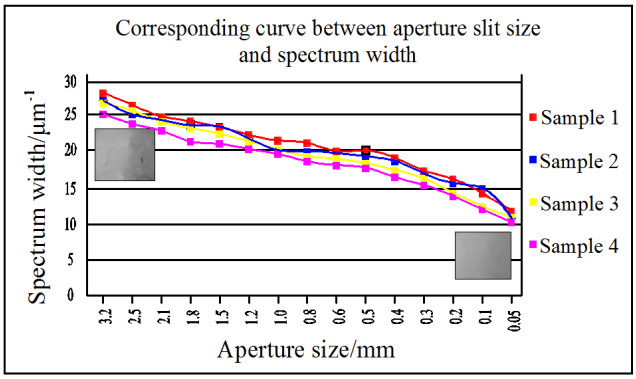

FIGURE 7. Relationship curve between aperture slit size and spectrum width.

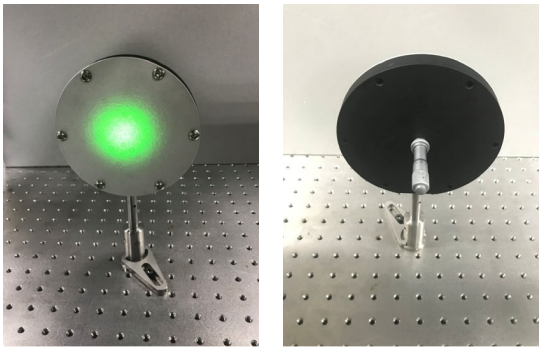

FIGURE 8. The experimental object of metal aluminium plate.

size can be controlled by changing the aperture size in the DSPI system.

A. EXPERIMENTAL SAMPLE

In the paper, the pigs ex vivo tibiae and femur are used as experimental sample to prove the effect of size of speckles on quality of speckle patterns in DSPI applied to strain detection of bioactive materials.

In order to ensure the activity of the detected object, all the experimental samples are taken from living organisms and placed in a non-culture environment no more than two hours. At the same time, in order to minimize the measurement error caused by soft tissue, this tissue should be removed as much as possible before detection experiment. The selected bone samples (sample number: #1∼#4) are given in Figure 4 (red rectangle selected area is the observation area).

B. SPECKLE STABILITY TEST UNDER DIFFERENT APERTURE SLIT SIZE

By using the DSPI experimental device shown in Figure 3, the stability of speckle image come from bone samples was measured under 15 different aperture slit sizes, and continuous 64 images were acquired for calculating the *IM* every time. For ensuring the samples with same activity in each test, each test sample will be taken out of the culture medium for no more than one hour before loading strain test. The monitoring results are shown in Figure 5.

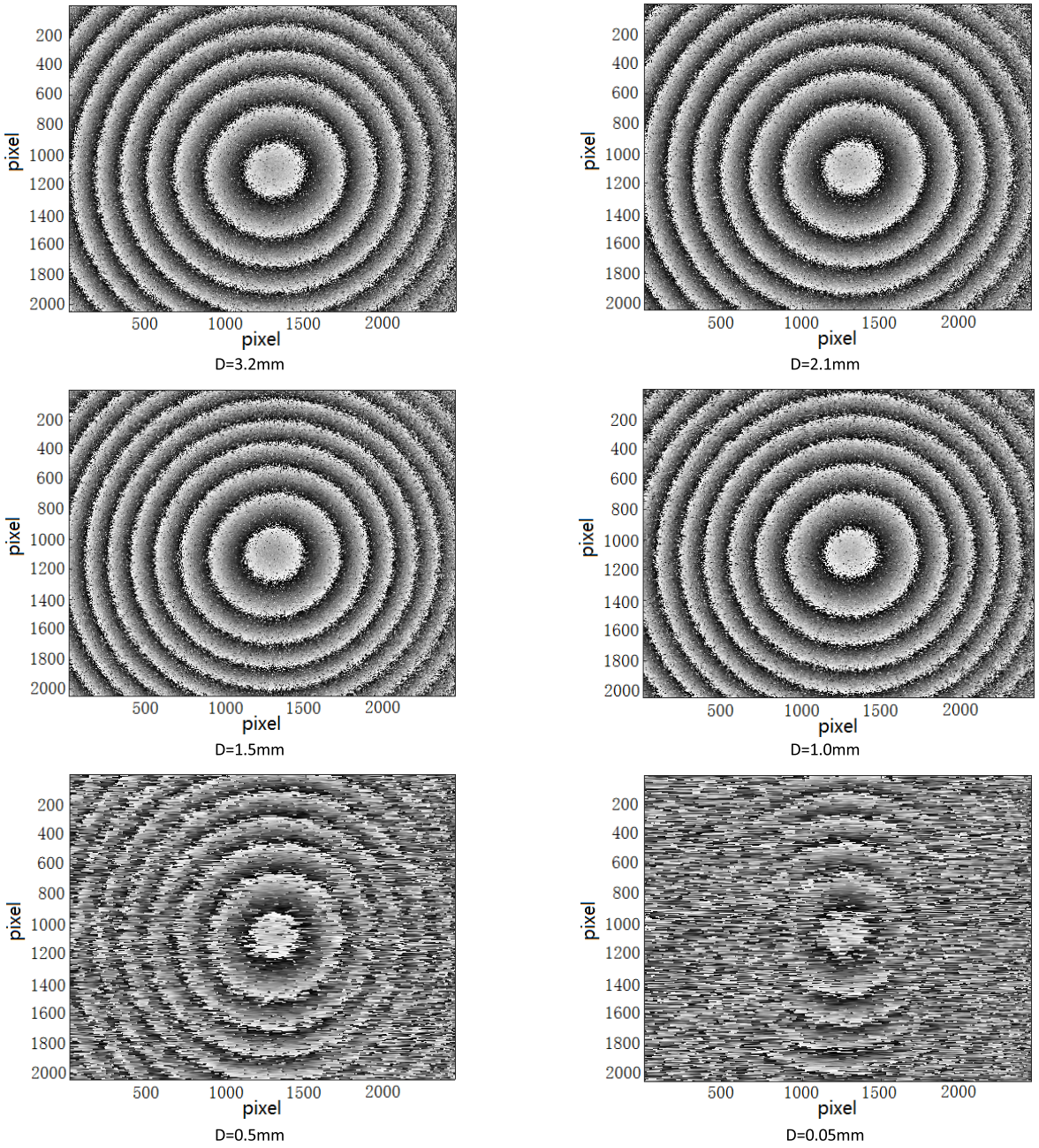

FIGURE 9. The phase maps of aluminum plate corresponding to same displacement loading under different aperture slit size.

As shown in Figure 5, with the aperture slit size becoming smaller, the speckle pattern becomes more stable, which proves that a bigger speckle size have a positive influence on stability of speckle patterns in continuous time. However, when the aperture size becomes larger, the size of speckles becomes smaller and the stability of speckle image becomes worse, which will weaken the correlation between pre-deformation speckle pattern and post-deformation speckle pattern. Therefore, a smaller aperture slit size for restraining speckle de-correlation is a better choice.

In the course of experiment, for avoiding the variety of light intensity caused by the change of aperture slit size, the output power of the laser is adjusted to ensure that the speckle image with same light intensity under different aperture slit size.

C. CONTRAST ASSESSMENT OF SPECKLE PATTERN

As mentioned above, the smaller aperture slit size means that the speckle pattern carries less information. What is more, for the strain detection with DSPI, it means that the quality of the phase map became worse and will make the subsequent strain detection difficult. Therefore, it is very necessary to evaluate the contrast of the speckle pattern. In the experiment, the four groups of experimental samples shown

in Figure 4 are taken as the research object. For each group of experimental objects, speckle patterns with different speckle size are obtained by changing the size of aperture slit in DSPI system, and the contrast of the speckle patterns is analyzed. Figure 6 shows the parts of speckle patterns obtained with different aperture slit size from 0.05 to 3.2 mm.

From Figure 6, we can see that large aperture size will produce smaller speckle grains, and the obtained speckle patterns will become clearer. Based on the evaluation method for the quality of speckle pattern described above, the corresponding power spectrum can be calculated. The larger the slit size of the aperture is, the wider the power spectrum of the speckle image is. The relationship between the spectral width and the aperture slit size is shown in Figure 7.

It can be seen from Figure 7, when the aperture slit size is 3.2mm, the gray level of the speckle pattern changes drastically. At this time, the power spectrum of the image is the widest. As the size of the aperture decreases, the power spectrum width becomes narrower and narrower. When the aperture slit size is 0.05 mm, the gray level of the speckle pattern changes slowly, and the corresponding power spectrum width is only $7\mu m^{-1}$. It is proved that as the speckle size increases, the variety of speckle pattern becomes more and more slowly, the corresponding power spectrum width decreases, and the contrast of the speckle pattern gets worse. This is because the larger speckle size can reduce the spatial cut-off frequency of the Fourier domain, resulting in subsequent degradation of the phase image quality in DSPI. Therefore, the size of speckles is critical for speckle measurement techniques and it is directly related to spatial resolution. In terms of acquiring image information, it has great significance to set larger aperture slit size which can make speckle patterns carry more information.

V. EFFECT OF THE SIZE OF SPECKLES ON STRAIN DETECTION OF INACTIVE AND ACTIVE MATERIALS

From the above experiments, it can be seen that the choice of speckle size is very important for the DSPI system applied to strain detection of bioactive materials. In fact, for the strain detection of inactive biomaterials, we can calculate the optimal aperture slit size according to the relevant parameters of the designed DSPI system, so as to obtain the best phase image. But for the strain detection of bioactive materials, due to the influence of surface activity, how to obtain the optimal size of aperture slit needs to be studied through experiments. If the slit width is too small, larger speckle particles can be obtained which can make the speckle pattern stable, and the correlation between the pre-deformation and post-deformation of speckle patterns is strong. However, due to the poor contrast of speckle pattern, the system may not be able to detect strain. On the contrary, if the aperture slit is too wide, a smaller size of speckle will be produced. Although the richer information can be acquired from speckle patterns, the increase of the instability of speckle patterns will lead to the serious noise caused by the de-correlation of speckle patterns, which will make the phase information

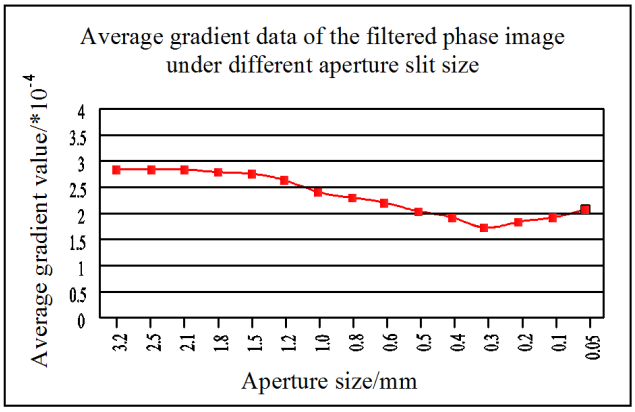

FIGURE 10. The average gradient value of filtered phase maps under different aperture slit sizes.

submerged in the noise. Therefore, it is very important to evaluate whether there is a compromise between the stability and the contrast of speckle image by choosing the optimal aperture slit size (speckle size) in DSPI system.

In the following experiments, we used two groups of experimental samples, non-active aluminum plate and active biomaterials, to study the quality of phase maps from the pre-deformation and post-deformation speckle pattern under the same loading conditions, respectively, which can prove the optimal speckle size is different when DSPI is applied to strain detection of inactive and active materials. In the following experiments, the quality of phase image is evaluated by calculating the average gradient of filtered phase maps [53].

A. DETECTION EXPERIMENT OF INACTIVE MATERIALS

Firstly, the strain of inactive metal materials is detected by using the DSPI system designed in this paper. In the experiment, the experimental device of DSPI is shown in Figure 3. Aluminum metal plate will be used as a substitute for bioactive biomaterials. In order to achieve spectrum separation, the range of spectrum should be expanded as far as possible, so as to maximize the signal-to-noise ratio of phase images [43], [54]. Therefore, under the condition of formula (3), maximum critical value of aperture slit is the optimal slit size for the strain detection system of DSPI. According to the sampling theorem, the maximum spatial frequency that the camera can recorded image information can be expressed as $f_{max} = 1/2d_{pixel}$ and the carrier frequency can be expressed as $f_{carrier} = sin\beta/\lambda$. So, from formula (3), we can get:

$$\beta \leq \arcsin(\lambda/3d_{pixel}), \tag{9}$$

Among them, β is the shear angle, λ is the laser wavelength, and d_{pixel} is the pixel size.

By substituting the above relationship into the experimental system of DSPI designed in this paper, the shear angle β in the experimental system can be calculated, and should satisfy the following conditions:

$$\beta < 2.946^{\circ} \tag{10}$$

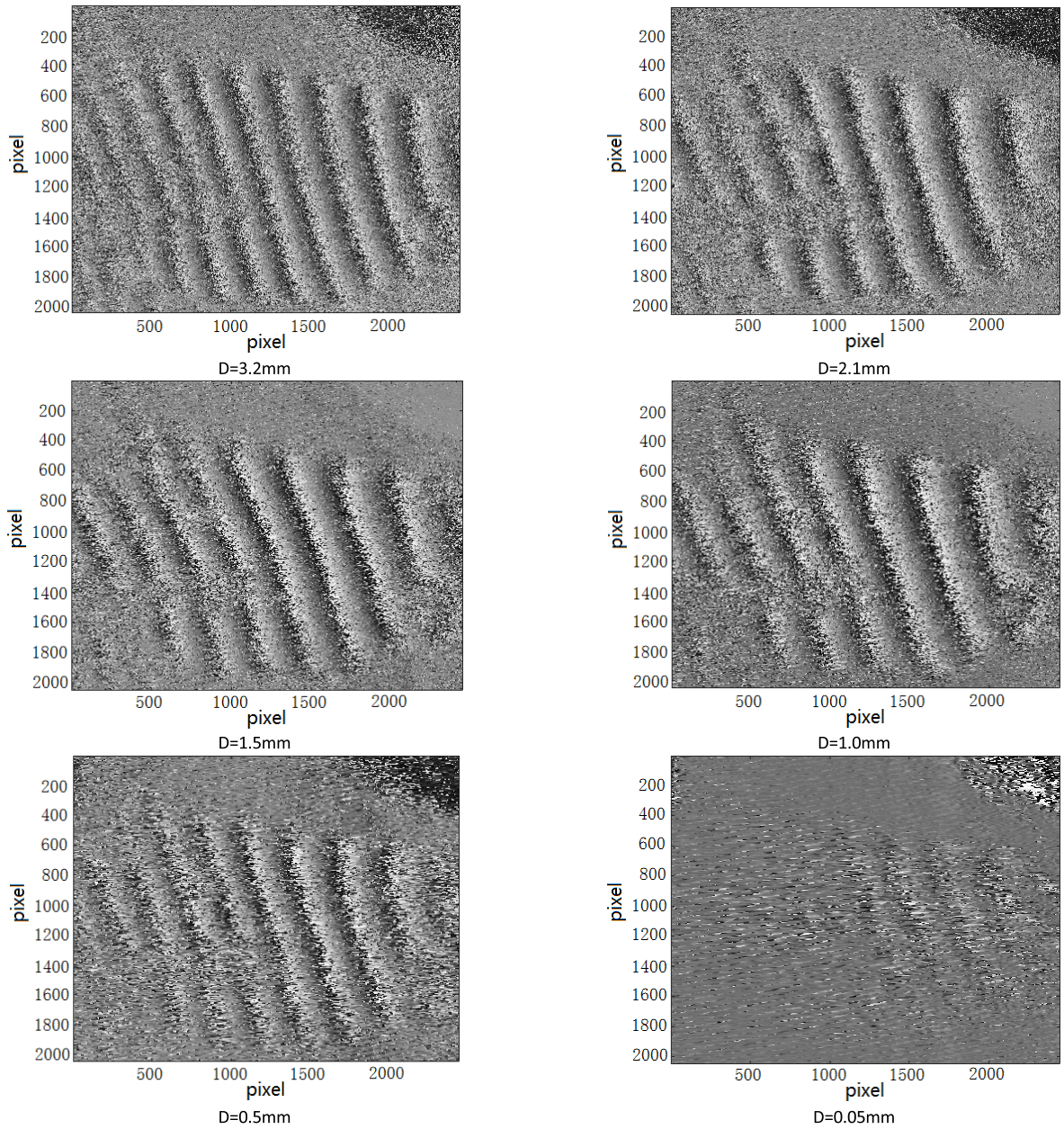

FIGURE 11. The phase maps of sample 1 corresponding to 5μm displacement loading under different aperture slit size.

At the same time, the relationship between the aperture slit size and shear angle β can be deduced from formula (3) when $4f_s$ is less than $f_{carrier}$.

At the same time, the relationship between the aperture size and the shear angle can also be deduced from the $4f_s \leq f_{carrier}$ in formula (3).

$$D \leq 1.22 \times f \times \sin \beta/2, \tag{11}$$

where, f is lens focal length and D is slit size. The size of the aperture size needs to satisfy the conditions:

$$D \leq 3.1365mm \tag{12}$$

According to the optimal slit selection theory of the above-mentioned DSPI system, when the DSPI designed is applied to the detection of inactive materials, we can obtain the maximum spectrum range by setting D to 3.1365 mm, then the best phase image quality can be obtained. In order to verify the above theory, the metal aluminium plate is used as the experimental object as shown in Figure 8. (The center of circular aluminium plate is loaded with micrometers).

Using the strain detection system of DSPI designed in this paper, the quantitative strain loading experiments of aluminum plate specimens were carried out under different aperture slit sizes. Fig.9 shows the phase images before and after deformation came from different aperture sizes under the same loading conditions.

According to Fig. 9, when the slit size satisfies spectrum separation, the larger the slit, the better the phase

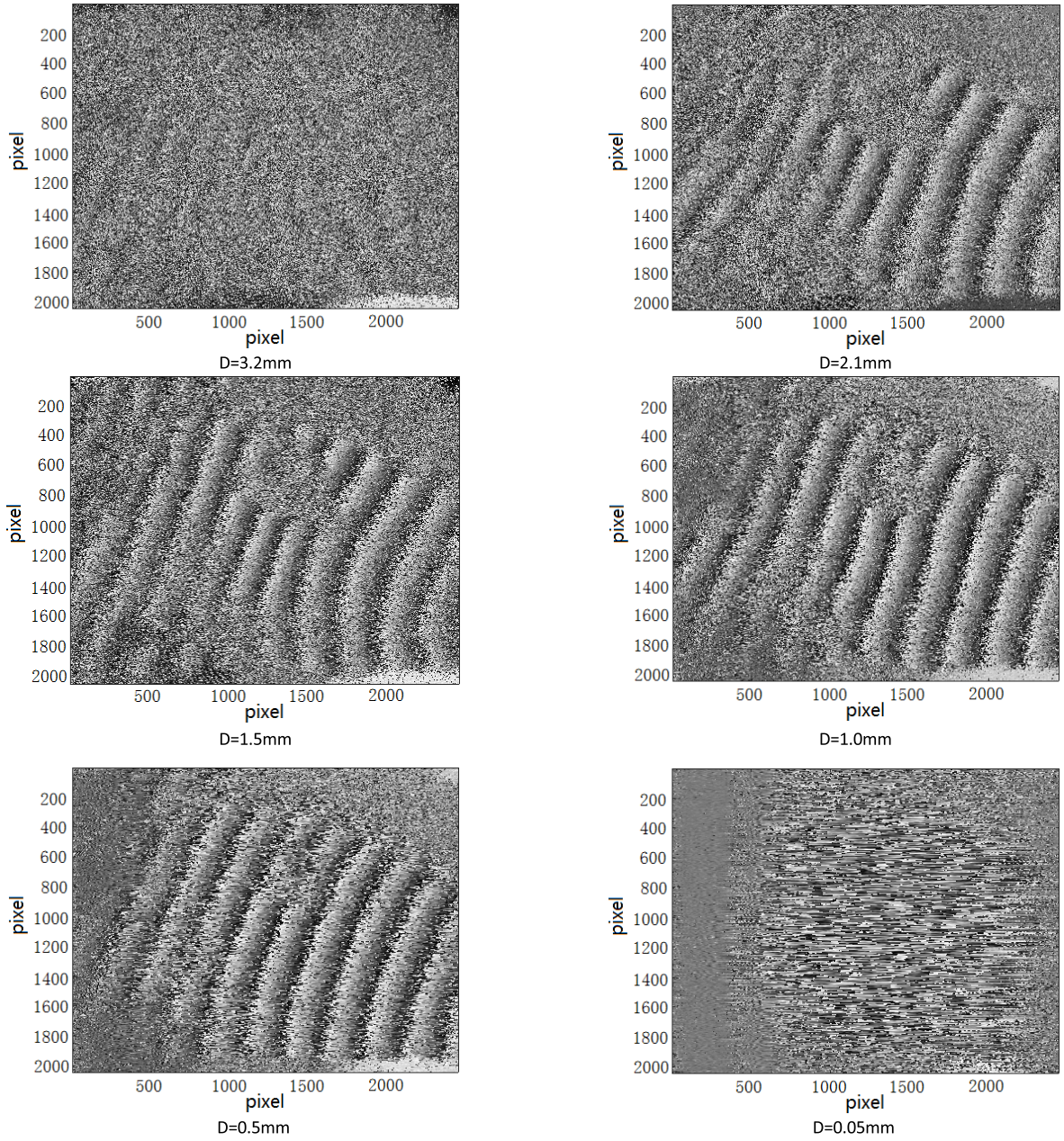

FIGURE 12. The phase maps of sample 2 corresponding to 5μm displacement loading under different aperture slit size.

image quality. As stated in some reports [55], [56], gradient features are basic and inherent properties of human visual perception that are commonly used to characterize the various of an image, and the average gradients can be used to characterize the overall quality of the image. In order to evaluate the quality of different phase images more objectively and accurately, all phase images are preprocessed by the same filtering method and then the average gradients are calculated, respectively. The experimental results are shown in Fig. 10.

It can be seen from Fig.9 and Fig.10 that the size of aperture should be as large as possible to obtain better phase image quality as long as the critical condition of spectrum separation (e.g., the slit size of this experimental device is about 3.2mm) is satisfied when the DSPI system is applied to strain detection of inactive materials such as metals, etc. This is mainly because when DSPI is applied to strain detection of inactive materials, the phenomenon of speckle image decorrelation becomes a secondary factor affecting the quality of speckle pattern due to the inactivity of the surface of the testing materials, and the contrast of the images becomes the main factor. Therefore, on the premise of satisfying the spectrum separation, the bigger the size of slit, the better the quality of phase image is. So the average gradient decreases with the decrease of the slit size generally.

At the same time, we can also see from Fig. 10 that when the slit size is about less than 0.3mm, because the amount of information carried by the speckle patterns too little, the ideal phase image can't be obtained. In this case, the image noise will lead to the discontinuity of the phase and the abrupt change of the fringes in the image, resulting in the increase of the average gradient value of the phase image, in which the average gradient value will can't be used to evaluate the quality of the image.

B. DETECTION EXPERIMENT OF ACTIVE MATERIALS

Using the same experimental device shown in Figure 3, the loading strain detection experiments of bone samples were carried out under different aperture slit sizes. The loading mode is side displacement loading, and the displacement is 5μm each time. Fig.11 shows the phase maps of sample #1 corresponding to 5μm displacement loading under different aperture slit size from 0.05mm to 3.2mm and Fig.12 shows the phase maps of sample #2 corresponding to 5μm displacement loading under different aperture slit size from 0.05mm to 3.2mm.

According to the Fig.11 and Fig.12, the phase map quality is evaluated by calculating the average gradient of the image. Similarly, we first process all phase maps with the same filter, and then calculate their average gradient. The experimental results of four groups of samples are shown in Figure 13.

It can be seen from Figure 13, for the strain detection of active bones under physiological conditions in DSPI, the average gradient increases first and then decreases with the reduction of the slit size, and the variation of average gradient can be divided into a rising process and a falling process. In the rising process (the slit size is from about 3.2 mm to 1.2 mm), the quality of the phase image is mainly affected by the stability of the speckle pattern because of the activity of the detection object. With the decrease of the size of the aperture slit, the stability of the speckle pattern generated by the system increases, which improves the quality of the phase image. Conversely, in the falling process (the slit size is reduced from about 1.2 mm to 0.05 mm)

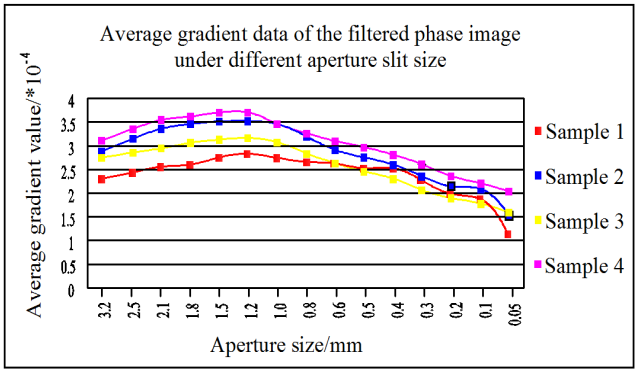

FIGURE 13. The average gradient value of filtered phase maps under different aperture slit sizes.

in which the size of the aperture slit has been reduced to a certain critical value, the speckle particles generated by the system will make the stability of the speckle pattern meet the correlation requirements before and after deformation. At this time, the amount of information contained in the speckle pattern will be the main factor affecting the quality of the phase image. Therefore, with the decrease of aperture slit, the amount of information of speckle pattern decreases, which will result in a decrease in the quality of the phase image.

So the optimal aperture slit size is not the maximum size in which the speckle pattern carries the richest amount of information. The main reason is that the size of the aperture slit is too large and the speckle size is small, which makes the speckle pattern too sensitive to detect the disturbance on the surface of the bioactive materials, and leads to the instability of the speckle pattern. Therefore, it is necessary to reduce the size of the aperture slit size to produce larger speckle particles, so as to improve the stability of the speckle image. When the aperture slit size is between 1.0 mm and 1.5 mm, the phase pattern quality is the best, which means the compromise between speckle stability and speckle image information is reached. At this time, the speckle size is the optimal size in DSPI.

VI. CONCLUSION

Through the above research, it can be seen that the optimal speckle size in DSPI is different when it is applied to different detection objects. For most inactive engineering materials, such as metal materials, its surface properties are stable for the absence of physiological environment and the speckle patterns between pre-deformation and post-deformation have strong correlation, so the speckle size should be as smaller as possible based on the premise of satisfying the sampling theorem and spectrum separation to obtain the maximum spectrum range.

When the application of DSPI technology to the strain detection of bioactive materials, with the changes of external environment, the movement of water molecules promotes molecular layer fluctuation on the biological tissue surface and the original physiological balance is constantly being broken with environment change, and a large amount of biological water on the complex contour interface will fluctuates drastically. At the same time, with the process of dewetting, the ultra-thin biological water layer will produce a large amount of film rupture and shrinkage. These changes will lead to serious de-correlation of speckle pattern. In this case, in order to select the ideal speckle size, it is necessary to evaluate whether there is any compromise between the amount of information and the stability of the speckle pattern, so as to obtain the best phase image.

However, when the DSPI system is applied to the surface strain detection of active biomaterials in physiological state, the change of unstructured environment will seriously affect the stability of speckle pattern which will lead to de-correlation of speckles before and after deformation. The interaction between nonlinearity and disorder is one of the

most challenging problems in complex optics. Therefore, how to establish the optimal speckle size constraint model through the parameters of the DSPI system and the characteristics of the detection object still need to be further explored.

REFERENCES

[1] C. Arvieux and H. Common, "New diagnostic tools for prosthetic joint infection," *Orthopaedics Traumatol., Surg. Res.*, vol. 26, pp. 1–43, Feb. 2019. doi: 10.1016/j.otsr.2018.04.029.

[2] H. C. Cheng, B. Y. Peng, M. S. Chen, C. F. Huang, Y. Lin, and Y. K. Shen, "Influence of deformation and stress between bone and implant from various bite forces by numerical simulation analysis," *Biomed Res. Int.*, vol. 35, May 2017, Art. no. 2827953. doi: 10.1155/2017/2827953.

[3] X. Xu, D. Luo, C. Guo, and Q. Rong, "A custom-made temporomandibular joint prosthesis for fabrication by selective laser melting: Finite element analysis," *Med. Eng. Phys.*, vol. 46, pp. 1–11, Aug. 2017. doi: 10.1016/j.medengphy.2017.04.012.

[4] Y. Wang, Z. Li, D. W. C. Wong, C. K. Cheng, and M. Zhang, "Finite element analysis of biomechanical effects of total ankle arthroplasty on the foot," *J. Orthopaedic Transl.*, vol. 12, pp. 55–65, Jan. 2017. doi: 10.1016/j.jot.2017.12.003.

[5] J. N. Wood, M. K. Henry, R. P. Berger, D. M. Lindberg, J. D. Anderst, L. Song, R. Localio, and C. Feudtner, "Use and utility of skeletal surveys to evaluate for occult fractures in young injured children," *J. Amer. Med. Directors Assoc.*, vol. 18, pp. 428–437, May/Jun. 2019. doi: 10.1016/j.acap.2018.08.007.

[6] S. Deane, N. P. Avdelidis, C. Ibarra-Castanedo, H. Zhang, H. Y. Nezhad, A. A. Williamson, T. Mackley, M. J. Davis, X. Maldague, and A. Tsourdos, "Application of NDT thermographic imaging of aerospace structures," *Infr. Phys. Technol.*, vol. 97, pp. 456–466, Mar. 2019. doi: 10.1016/j.infrared.2019.02.002.

[7] A. Bendada, S. Sfarra, M. Genest, D. Paoletti, S. Rott, E. Talmy, C. Ibarra-Castanedo, and X. Maldague, "How to reveal subsurface defects in Kevlar composite materials after an impact loading using infrared vision and optical NDT techniques?" *Eng. Fract. Mech.*, vol. 108, pp. 195–208, Aug. 2013. doi: 10.1016/j.engfracmech.2013.02.030.

[8] R. Kulkarni and P. Rastogi, "Simultaneous estimation of multiple phases in digital holographic interferometry using state space analysis," *Opt. Lasers Eng.*, vol. 104, pp. 109–116, May 2018. doi: 10.1016/j.optlaseng.2017.08.016.

[9] Y. Fang, S. J. Wu, and L. X. Yang, "Synchronous measurement of three-dimensional deformations using tri-channel spatial-carrier digital speckle pattern interferometry," *Appl. Mech. Mater*, vol. 868, pp. 316–322, Jul. 2017. doi: 10.4028/www.scientific.net/AMM.868.316.

[10] H. Lopes, J. V. A. dos Santos, and P. Moreno-García, "Evaluation of noise in measurements with speckle shearography," *Mech. Syst. Signal Process.*, vol. 118, pp. 259–276, Mar. 2019. doi: 10.1016/j.ymssp.2018.08.042.

[11] J. Song, J. Yang, F. Liu, and K. Lu, "High temperature strain measurement method by combining digital image correlation of laser speckle and improved RANSAC smoothing algorithm," *Opt. Lasers Eng.*, vol. 111, pp. 8–18, Dec. 2018. doi: 10.1016/j.optlaseng.2018.07.012.

[12] J. R. Tyrer, "Electronic speckle pattern interferometry," *Opt. Meas. Methods Biomech.*, vol. 11, no. 1, pp. 99–124, Jan. 1987. doi: 10.1007/978-0-585-35228-2_6.

[13] W. An and T. E. Carlsson, "Speckle interferometry for measurement of continuous deformations," *Opt. Lasers Eng.*, vol. 40, pp. 529–541, Nov./Oct. 2003. doi: 10.1016/S0143-8166(02)00085-4.

[14] M. Kumar and C. Shakher, "Measurement of temperature and temperature distribution in gaseous flames by digital speckle pattern shearing interferometry using holographic optical element," *Opt. Lasers Eng.*, vol. 73, pp. 33–39, Oct. 2015. doi: 10.1016/j.optlaseng.2015.04.002.

[15] M. Kumar, R. Agarwal, R. Bhutani, and C. Shakher, "Measurement of strain distribution in cortical bone around miniscrew implants used for orthodontic anchorage using digital speckle pattern interferometry," *Proc. SPIE*, vol. 55, no. 5, May 2016, Art. no. 054101. doi: 10.1117/1.OE.55.5.054101.

[16] P. Aswendt, R. Höfling, and W. Totzauer, "Digital speckle pattern interferometry applied to thermal strain measurements of metal-ceramic compounds," *Opt. Laser Technol*, vol. 22, pp. 278–282, Aug. 1990. doi: 10.1016/0030-3992(90)90061-8.

[17] P. Sun, "Evaluation of two-dimensional displacement components of symmetrical deformation by phase-shifting electronic speckle pattern interferometry," *Appl. Opt.*, vol. 46, no. 15, pp. 2859–2862, 2007. doi: 10.1364/AO.46.002859.

[18] P. P. Padghan and K. M. Alti, "Quantification of nanoscale deformations using electronic speckle pattern interferometer," *Opt. Laser Technol.*, vol. 107, pp. 72–79, Nov. 2018. doi: 10.1016/j.optlastec.2018.05.019.

[19] K. Kim, T. Choi, M. Na, and H. Jung, "Residual stress measurement on the butt-welded area by electronic speckle pattern interferometry," *Nucl. Eng. Technol.*, vol. 47, pp. 115–125, Feb. 2015. doi: 10.1016/j.net.2014.09.001.

[20] G. Pedrini, V. Martínez-García, P. Weidmann, M. Wenzelburger, A. Killinger, U. Weber, S. Schmauder, R. Gadow, and W. Osten, "Residual stress analysis of ceramic coating by laser ablation and digital holography," *Exp. Mech.*, vol. 56, no. 5, pp. 683–701, Jun. 2015. doi: 10.1007/s11340-015-0120-3.

[21] C. Dong, K. Li, Y. Jiang, D. Arola, and D. Zhang, "Evaluation of thermal expansion coefficient of carbon fiber reinforced composites using electronic speckle interferometry," *Opt. Express*, vol. 26, pp. 531–543, 2018. doi: 10.1364/OE.26.000531.

[22] M. Kumar and C. Shakher, "Experimental characterization of the hygroscopic properties of wood during convective drying using digital holographic interferometry," *Appl. Opt.*, vol. 55, no. 5, pp. 960–968, 2016. doi: 10.1364/AO.55.000960.

[23] C. G. T. Ruiz, M. H. De La Torre-Ibarra, J. M. Flores-Moreno, C. Frausto-Reyes, and F. M. Santoyo, "Cortical bone quality affectations and their strength impact analysis using holographic interferometry," *Biomed. Opt. Express*, vol. 9, pp. 4818–4833, 2018. doi: 10.1364/BOE.9.004818.

[24] C. Dudescu, J. Naumann, M. Stockmann, and S. Nebel, "Characterisation of thermal expansion coefficient of anisotropic materials by electronic speckle pattern interferometry," *Strain*, vol. 42, no. 3, pp. 197–205, Aug. 2006. doi: 10.1111/j.1475-1305.2006.00271.x.

[25] M. Kumar, K. K. Gaur, and C. Shakher, "Measurement of material constants (young's modulus and Poisson's ratio) of polypropylene using digital speckle pattern interferometry (DSPI)," *Jpn. Soc. Exp. Mech.*, vol. 15, pp. s87–s91, Aug. 2015. doi: 10.11395/jjsem.15.s87.

[26] L. Bruno, L. Pagnotta, and A. Poggialini, "Laser speckle decorrelation in NDT," *Opt. Lasers Eng.*, vol. 34, pp. 55–65, Jun. 2000. doi: 10.1016/S0143-8166(00)00057-9.

[27] M. B. Bernini, A. Federico, and G. H. Kaufmann, "Noise reduction in digital speckle pattern interferometry using bidimensional empirical mode decomposition," *Appl. Opt.*, vol. 47, no. 14, pp. 2592–2598, 2008. doi: 10.1364/AO.47.002592.

[28] Y. Tounsi, M. Kumar, A. Nassim, and F. Mendoza-Santoyo, "Speckle noise reduction in digital speckle pattern interferometric fringes by nonlocal means and its related adaptive kernel-based methods," *Appl. Opt.*, vol. 57, no. 27, pp. 7681–7690, 2018. doi: 10.1364/AO.57.007681.

[29] P. Memmolo, M. Iannone, M. Ventre, P. A. Netti, A. Finizio, M. Paturzo, and P. Ferraro, "Quantitative phase maps denoising of long holographic sequences by using SPADEDH algorithm," *Appl. Opt.*, vol. 52, pp. 1453–1460, 2013. doi: 10.1364/AO.52.001453.

[30] G. R. Gaudette, J. Todaro, I. B. Krukenkamp, and F.-P. Chiang, "Computer aided speckle interferometry: A technique for measuring deformation of the surface of the heart," *Ann. Biomed. Eng.*, vol. 29, no. 9, pp. 775–780, Sep. 2001. doi: 10.1114/1.1397785.

[31] P. Zhong, Z. Li, H. Yang, X. Tang, and G. He, "A strain distribution sensing system for bone-implant interfaces based on digital speckle pattern interferometry," *Sensors*, vol. 19, pp. 365–378, Jan. 2019. doi: 10.3390/s19020365.

[32] J. M. Huntley, "Random phase measurement errors in digital speckle pattern interferometry," *Opt. Lasers Eng.*, vol. 26, nos. 2–3, pp. 131–150, Jan./Feb. 1997. doi: 10.1117/12.211885.

[33] J. D. Briers, G. Richards, and X. W. He, "Capillary blood flow monitoring using laser speckle contrast analysis (LASCA)," *J. Biomed. Opt.*, vol. 4, pp. 164–175, Jan. 1999. doi: 10.1117/1.429903.

[34] S. Yuan, A. Devor, D. A. Boas, and A. K. Dunn, "Determination of optimal exposure time for imaging of blood flow changes with laser speckle contrast imaging," *Appl. Opt.*, vol. 44, no. 10, pp. 1823–1830, 2005. doi: 10.1364/AO.44.001823.

[35] M. N. Osipov and R. N. Sergeev, "Digital speckle photography with the ring aperture diaphragm," *Procedia Eng.*, vol. 201, pp. 155–163, Jan. 2017. doi: 10.1016/j.proeng.2017.09.591.

[36] D. Chicea, "Speckle size, intensity and contrast measurement application in micron-size particle concentration assessment," *Eur. Phys. J. Appl. Phys.*, vol. 40, pp. 305–310, Dec. 2007. doi: 10.1051/epjap:2007163.
[37] J. W. Goodman, "Speckle phenomena in optics: Theory and application," in *Roberts Company, Greenwood Village*. Englewood, CO, USA: Roberts & Company, 2007. doi: 10.1007/s10955-007-9440-8.
[38] Q. B. Li and F. P. Chiang, "Three-dimensional dimension of laser speckle," *Appl. Opt.*, vol. 31, no. 29, pp. 6287–6296, 1992. doi: 10.1364/AO.31.006287.
[39] M. Talbi and M. Brunel, "Interferometric particle sizing with overlapping images despite Moiré," *Opt. Commun.*, vol. 400, pp. 61–68, Oct. 2017. doi: 10.1016/j.optcom.2017.04.075.
[40] S. J. Kirkpatrick, D. D. Duncan, and E. M. Wells-Gray, "Detrimental effects of speckle-pixel size matching in laser speckle contrast imaging," *Opt. Lett.*, vol. 33, no. 24, pp. 2886–2888, 2008. doi: 10.1364/OL.33.002886.
[41] J. C. Ramirez-San-Juan, E. Mendez-Aguilar, N. Salazar-Hermenegildo, A. Fuentes-Garcia, R. Ramos-Garcia, and B. Choi, "Effects of speckle/pixel size ratio on temporal and spatial speckle-contrast analysis of dynamic scattering systems: Implications for measurements of blood-flow dynamics," *Biomed. Opt. Express*, vol. 4, no. 10, pp. 1883–1889, 2013. doi: 10.1364/BOE.4.001883.
[42] R. A. Braga and R. J. González-Peña, "Accuracy in dynamic laser speckle: Optimum size of speckles for temporal and frequency analyses," *Opt. Eng.*, vol. 55, May 2016, Art. no. 121702. doi: 10.1117/1.OE.55.12.121702.
[43] W. Steinchen and L. Yang, *Digital Shearography: Theory and Application of Digital Speckle Image Shearing Interferometry*. Bellingham, WA, USA: SPIE, 2003.
[44] P. P. Padghan and K. M. Alti, "Impact of multiple usages of digital filters on speckle contrast and phase maps," *Optik*, vol. 154, pp. 610–615, Feb. 2018. doi: 10.1016/j.ijleo.2017.10.073.
[45] M. D. Z. Ansari and A. K. Nirala, "Biospeckle activity measurement of Indian fruits using the methods of cross-correlation and inertia moments," *Optik*, vol. 124, pp. 2180–2186, Aug. 2013. doi: 10.1016/j.ijleo.2012.06.081.
[46] R. Arizaga, M. Trivi, and H. Rabal, "Speckle time evolution characterization by the co-occurrence matrix analysis," *Opt. Laser Technol.*, vol. 31, pp. 163–169, May 1999. doi: 10.1016/S0030-3992(99)00033-X.
[47] M. Z. Ansari and A. K. Nirala, "Assessment of bio-activity using the methods of inertia moment and absolute value of the differences," *Optik*, vol. 124, pp. 512–516, Mar. 2011. doi: 10.1016/j.ijleo.2011.12.013.
[48] A. Zdunek, A. Adamiak, P. M. Pieczywek, and A. Kurenda, "The biospeckle method for the investigation of agricultural crops: A review," *Opt. Lasers Eng.*, vol. 52, pp. 276–285, Jan. 2014. doi: 10.1016/j.optlaseng.2013.06.017.
[49] J. Semmlow, "The Fourier transform and power spectrum," in *Signals, and Systems for Bioengineers*. New York, NY, USA: Academic, 2012, pp. 253–268. doi: 10.1016/b978-0-12-384982-3.00004-3.
[50] W. V. Drongelen, "Lomb's Algorithm and multitaper power spectrum estimation," in *Signal Processing for Neuroscientists*. Washington, DC, USA: Heldref, 2018, pp. 153–180. doi: 10.1016/b978-0-12-810482-8.00008-4.
[51] R. Martin, "Noise power spectral density estimation based on optimal smoothing and minimum statistics," *IEEE Trans. Speech Audio Process.*, vol. 9, no. 5, pp. 504–512, Jul. 2001. doi: 10.1109/89.928915.
[52] F. J. Simois and J. J. Murillo-Fuentes, "On the power spectral density applied to the analysis of old canvases," *Signal Process.*, vol. 143, pp. 253–268, Feb. 2018. doi: 10.1016/j.sigpro.2017.08.006.
[53] L. Liu, Y. Hua, and Q. Zhao, H. Huang, and A. C. Bovik, "Blind image quality assessment by relative gradient statistics and adaboosting neural network," *Signal Process., Image Commun.*, vol. 40, pp. 1–15, Jan. 2015. doi: 10.1016/j.image.2015.10.005.
[54] Y. Wang, X. Gao, X. Xie, S. Wu, Y. Liu, and L. Yang, "Simultaneous dual directional strain measurement using spatial phase-shift digital shearography," *Opt. Lasers Eng.*, vol. 87, pp. 197–203, Dec. 2016. doi: 10.1016/j.optlaseng.2015.12.009.
[55] W. Zhou, L. Yu, W. Qiu, Y. Zhou, and M. Wu, "Local gradient patterns (LGP): An effective local-statistical-feature extraction scheme for no-reference image quality assessment," *Inf. Sci.*, vol. 40, pp. 397–398, Aug. 2017. doi: 10.1016/j.ins.2017.02.049.
[56] T. Sun, S. Ding, W. Chen, and X. Xu, "No-reference image quality assessment based on gradient histogram response," *Comput. Electr. Eng.*, vol. 54, pp. 330–344, Aug. 2016. doi: 10.1016/j.compeleceng.2015.11.007.

ZHISONG LI received the bachelor's and master's degrees from the Henan University of Science and Technology, Henan, China, in 2013. He is currently pursuing the Ph.D. degree with Donghua University, Shanghai, China. He is engaged in the research of optical sensors and optical metrology.

PING ZHONG received the bachelor's degree in computer science from Jilin University, Jilin, China, in June 1996, and the master's and Ph.D. degrees in optical engineering from the Chinese Academy of Sciences, Jilin, in June 2004. He is currently a Professor with Donghua University, Shanghai, China. His research interests include optical metrology, image processing, and optical sensors.

XIN TANG received the bachelor's degree in electronic and information engineering from the Shanghai University of Engineering Science. He is currently pursuing the master's degree in optical engineering with Donghua University. He is currently involved in the research of optical metrology, image processing, and optical sensors.

JIAYAO LING received the bachelor's degree in optoelectronic technology and science from Donghua University, where he is currently pursuing the master's degree in optical engineering. He is currently in the research of optical metrology, image processing, and optical sensors.

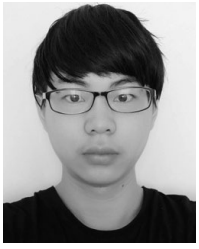

JIAWEI CHEN is currently pursuing the bachelor's degree in optical engineering with Donghua University. His research interests include optical metrology and optical sensors.

GUOXING HE received the bachelor's and master's degrees in physics from Fudan University, in April 1983 and December 1986, respectively. He is currently a Professor with Donghua University, Shanghai, China. His research interests include optical metrology and optical sensors.